Surface Science xxx (2014) xxx–xxx

Contents lists available at ScienceDirect

Surface Science

journal homepage: www.elsevier.com/locate/susc

Adsorption of thioether molecules on an alumina thin film

Yi Pan [a], Niklas Nilius [a,b,*], Wolf-Dieter Schneider [a,c], Hans-Joachim Freund [a]

[a] Fritz Haber Institute of the Max Planck Society, Faradayweg 4-6, 14195 Berlin, Germany
[b] Institute of Physics, Carl von Ossietzky University Oldenburg, 26111 Oldenburg, Germany
[c] École Polytechnique Fédérale de Lausanne, Institute of Condensed Matter Physics, CH-1015 Lausanne, Switzerland

ARTICLE INFO

Article history:
Received 25 April 2014
Received in revised form 28 May 2014
Accepted 30 May 2014
Available online xxxx

Keywords:
Molecule–oxide interactions
Scanning tunneling microscopy
Adsorption
Thioether-molecules
Aluminum oxide

ABSTRACT

Low-temperature scanning tunneling microscopy has been employed to study the adsorption of (bis(3-phenylthio)-phenyl)sulfane (BPPS) molecules on an aluminum-oxide film grown on NiAl(110). Large variations in the molecular coverage on incompletely oxidized samples indicate substantial differences in the binding strength of BPPS to metallic (NiAl) versus dielectric (alumina) surfaces. From atomically resolved images, we obtain possible BPPS adsorption geometries on the oxide, in which the sulfur centers and not the phenyl rings of the molecule govern the interaction. A local hexagonal ordering of BPPS, as deduced from pair correlation functions, suggests a preferential binding of the BPPS sulfur atoms to Al ions with distorted pyramidal coordination in the oxide surface. Our work provides insight into rarely explored binding schemes of organic molecules on wide-gap oxide materials.

1. Introduction

The interplay between organic molecules and metal surfaces has been already in the focus of research for several decades [1,2]. This continued interest is driven by various applications of molecular–metal interfaces, e.g. for new electronic, light-emitting and photovoltaic devices based on organic materials. The interaction of organic molecules and non-metallic surfaces, on the other hand, has attracted much less attention, although the technological relevance of this combination is equally large [3]. Interfaces between organic matter and oxide supports, for example, are of crucial importance for liquid–solid solar cells, in which the optical excitation occurs in molecular sensitizers, while separation and transport of the photo-generated carriers are realized by an oxide [4]. The most prominent example in this regard is the Grätzel cell, consisting of a TiO_2 powder covered with Dye-molecules, which has reached conversion efficiencies of 15% to date [5]. Molecule–oxide interfaces are of interest also in the widespread field of heterogeneous catalysis, where oxides are typically used as cheap and robust support materials [6–8].

The significance of molecule–oxide interfaces is in contrast to the limited research activities in the field. Despite a vital technological interest, fundamental studies on such systems are rare, a discrepancy that arises from several experimental difficulties. First of all, the binding between wide-gap insulators and common organic molecules is weak, as the interaction arises mostly from van-der-Waals and Coulomb forces and not from chemical bonds [9,10]. As a consequence, molecule–oxide junctions exhibit high structural flexibility at room temperature and defined interfaces only develop at cryogenic conditions. More relevant is the poor electrical conductivity of most molecule–oxide systems, which limits the applicability of electron-mediated spectroscopic and microscopic techniques [11]. Especially, the use of scanning tunneling microscopy (STM) for structural characterization at the nanometer scale is challenging, as the tip easily perturbs the weakly bound adsorbates [12–15]. Closely related to the issue of finite conductivity are the unusual imaging properties of molecules in the STM. In many cases, molecular orbitals contribute only weakly to the STM image contrast, as they poorly overlap with the substrate electronic states and cannot serve as initial or final state in a tunneling process.

In this study, we have overcome these restrictions by using an oxide film, thin enough to maintain a finite conductivity, to support the organic molecules. Our model system is alumina, an archetypical ionic insulator with 8 eV band gap, grown on a NiAl(110) substrate [16,17]. Our probe molecule, a thioether compound consisting of four phenyl rings linked by sulfur atoms, has recently attracted attention as it was found to act as re-dispersion agent for metal nanoparticles [18,19]. On the basis of atomically resolved STM images, we will determine the binding behavior of the molecules on the oxide surface and analyze general aspects of molecule–oxide interactions.

* Corresponding author at: Fritz Haber Institute of the Max Planck Society, Faradayweg 4-6, 14195 Berlin, Germany.
E-mail address: nilius@fhi-berlin.mpg.de (N. Nilius).

http://dx.doi.org/10.1016/j.susc.2014.05.021
0039-6028/

2. Experiment

The experiments have been performed with a custom-built ultra-high vacuum STM operated at 4.5 K. The alumina films were prepared by oxidizing a sputtered and annealed NiAl(110) single crystal in 5 $\times 10^{-6}$ mbar of oxygen at 550 K, followed by a vacuum-annealing step at 1000 K [17]. The film quality was routinely checked with low-energy-electron-diffraction, exhibiting a complex yet sharp spot pattern, and STM measurements revealing wide, atomically-flat oxide terraces. The main properties of the NiAl-supported alumina films have been discussed in several papers before and shall only be sketched at this point [20,21]. The film comprises four atomic layers; (i) an interfacial Al_i plane consisting of atoms in pentagonal and heptagonal configuration, (ii) a hexagonal O_i plane, (iii) an iso-structural Al_s plane and (iv) a terminating O_s plane made of triangular and square units (Fig. 1a). While each interface Al_i ion has three O neighbors, the Al_s coordination number varies between four and five due to ions in tetrahedral and pyramidal sites [20]. The oxide lattice is composed of rectangular unit cells (10.7 × 17.9 Å^2), being arranged in two reflection domains rotated by ±24° against the lattice of the NiAl support [22]. The oxide has a commensurate relationship with the substrate only along the NiAl[$1\bar{1}0$] direction, while no commensurability exists along the orthogonal NiAl[001]. In order to release misfit strain in the commensurate direction, a periodic network of dislocation lines is inserted into the film, comprising both antiphase and reflection boundaries between equal and mirrored surface domains, respectively [23]. The boundaries appear as protruding lines in empty-state STM images, as they possess a set of unoccupied defect states in the oxide band [24].

The adsorption experiments were carried out with (bis(3-phenylthio)-phenyl)sulfane (referred to as BPPS in the following), synthesized in the group of Prof. Blechert at the Technical University Berlin [18,25]. The compound consists of four phenyl rings linked via three sulfur atoms in meta-positions. Due to facile rotation about the C-S-C axes, a variety of configurations of the molecule can be realized upon adsorption, e.g. the chain-like and folded conformers shown in Fig. 1b–d. The molecules were purified by extensive degassing at 430 K and dosed from an alumina crucible onto the fresh oxide film at 300 K. Immediately after deposition, the samples were transferred into the cryogenic microscope to avoid contamination.

3. Results and discussion

On incompletely oxidized surfaces, the BPPS molecules show a high preference for binding to the metallic NiAl, while the coexisting oxide patches remain essentially empty (Fig. 2a). This difference in sticking indicates a much stronger BPPS adhesion onto metallic than dielectric surfaces, reflecting the chemical inertness of the latter. The observed variations in local coverage demonstrate also the high mobility of the molecules that are always able to reach a nearby NiAl patch at 300 K. By evaluating the mean distance between adjacent metal areas on samples with different metal–oxide surface ratio, we have determined the lower bound for the BPPS diffusion length on the oxide film to be of the order of 500 nm [26]. A detailed discussion of thioether molecules interacting with a NiAl surface can be found in the literature [18].

On fully oxidized samples, a molecular fingerprint becomes detectable also on the alumina film (Fig. 2b). Atom-sized protrusions of ~0.5 Å height and 5–7 Å diameter are found on defect-free oxide domains and, less abundant, along the domain boundaries (bright lines in Fig. 2b). Already a crude image inspection reveals that the maxima are not randomly distributed, but form a hexagonal pattern on the surface. Typical distances are derived from pair-correlation functions, calculated on the basis of STM images as shown in Figs. 2b. Three characteristic separations between the maxima are revealed, namely (10 ± 1), (22 ± 5) and (45 ± 5) Å (Fig. 3). Also the connecting lines between the protrusions have distinct orientations, following the diagonals of the unit cells in the two oxide domains (see arrows in Fig. 2b for one domain). Note that molecules located directly on the domain boundaries have been excluded from this statistics, as their positions might be altered by the line defects.

The adsorption pattern observed on the alumina film seems incompatible with the structure of the BPPS molecules at first glance. Assuming that either the phenyl rings or the sulfur atoms become visible in the STM, we would expect to find either four or three maxima in linear, triangular or rhomboidal configuration to represent a single molecule (Fig. 1b–d). In contrast, most protrusions appear in pairs with either 10 or 22 Å distance, suggesting that only some of the molecular entities actually contribute to the contrast. In a possible scenario, two sulfur atoms might be detected in the STM, while the third one remains invisible. A separation of 22 Å between adjacent maxima would then correspond to the first and last sulfur atom in linear BPPS

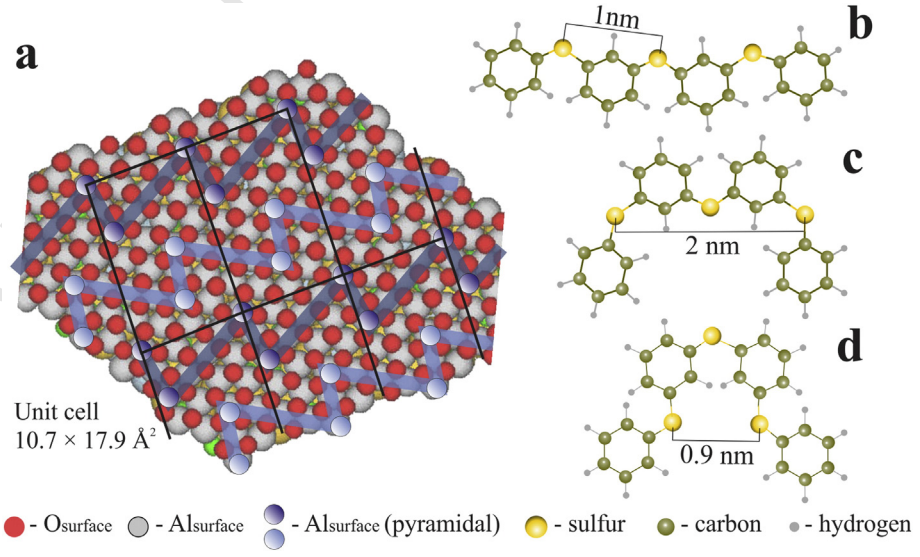

Fig. 1. (a) Ball model of the Al_s and O_s planes of the alumina film grown on NiAl(110). The Al_s ions in distorted (regular) pyramidal configuration are highlighted by blue balls (zig-zag lines), as they dominate the image contrast seen in STM. (b-d) Three planar conformations of the (bis(3-phenylthio)-phenyl)sulfane molecule. Note that various other 2D and 3D conformers exist and our selection is not exhaustive. (For interpretation of the references to color in this figure legend, the reader is referred to the web version of this article.).

Please cite this article as: Y. Pan, et al., Adsorption of thioether molecules on an alumina thin film, Surf. Sci. (2014), http://dx.doi.org/10.1016/j.susc.2014.05.021

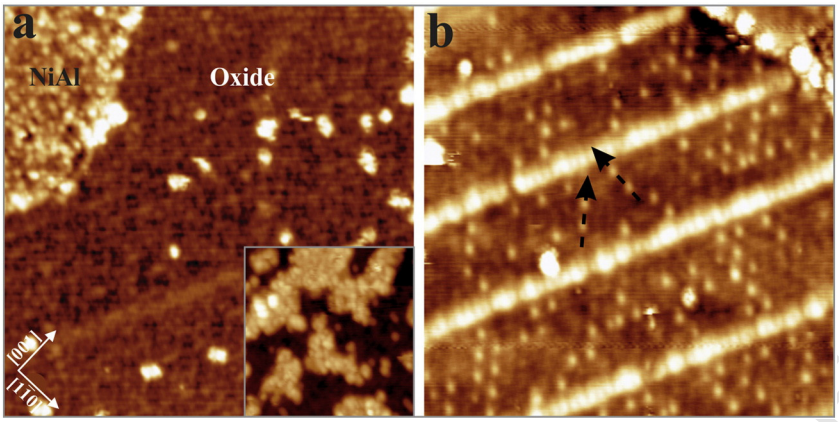

Fig. 2. STM topographic images of (a) a partly and (b) a fully-oxidized NiAl(110) surface after dosing BPPS molecules at room temperature (40×40 nm^2). Whereas molecules are densely-packed on the metal substrate (see inset and upper right corner in a), an open, hexagonal arrangement is observed on the alumina film. The bright lines represent the dislocation network that is better resolved at 2.5 V (b) than at 1.5 V (a) due to the energy position of characteristic defect states [24]. The arrows in (b) represent typical orientations of BPPS-related pairs on the alumina surface.

conformers (Fig. 1b), while 10 Å spacing would match two neighboring sulfurs either in linear or folded species (Fig. 1d). Alternatively, two out of the four phenyls might produce the observed contrast. In this case, maxima with 22 Å separation would represent the first and third phenyl ring of linear conformers or the terminal rings of folded ones (Fig. 1b,c), while a pairing of 10 Å would reflect two adjacent rings again. Note that the pair correlation function of Fig. 3 has its overall maximum at 22 Å, indicating that this separation is most frequently observed on the surface.

For reasons explained later, we propose that the sulfur atoms and not the phenyl rings determine the image contrast of BPPS molecules on the alumina film. This implies that only two out of three sulfurs are actually imaged in the STM, resulting in the tentative adsorption geometries depicted in Fig. 4. Two elongated molecules, each one represented by its outer S atoms, would be responsible for the contrast in panel (a) and account for the rhomboidal spot pattern. Conversely, two neighboring sulfur atoms might lead to the contrast seen in panel (b). On the basis of such models, even the local binding sites of the BPPS sulfur can be deduced from atomically resolved STM images of the alumina film. According to earlier work, the atomic protrusions seen in Fig. 4c are related to Al_s ions in the upper oxide bilayer [20]. The cations produce a characteristic zig-zag pattern, as the fivefold coordinated Al_s appear brighter than their fourfold counterparts (Figs. 1a, 4a–c). Moreover, two fivefold coordinated Al_s ion per unit cell stick out, as they sit in a strongly distorted pyramidal environment (large circles in Fig. 4c). Using them as internal markers, the position of the other Al_s ions and the detectable sulfur atoms can be reconstructed. Apparently, the S atoms of the BPPS exclusively bind to fivefold coordinated Al_s ions in the surface and neither to fourfold coordinated species or to O^{2-} ions. As the fivefold coordinated Al_s carry the highest positive charge of all surface ions, we propose that electrostatic and polarization forces dominate the interaction between the electronegative sulfur and the oxide cations.

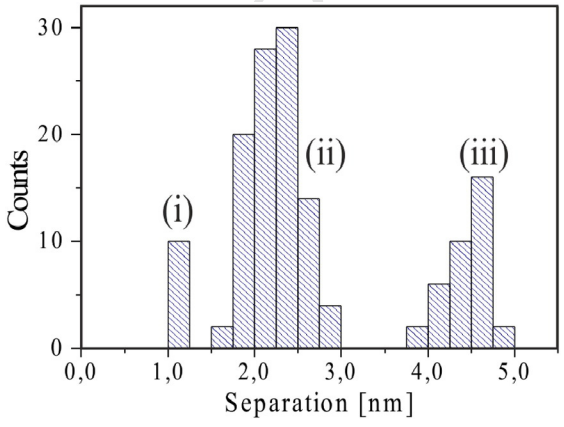

Fig. 3. Pair-correlation function obtained from several STM images of the BPPS-alumina system. The three maxima represent (i) molecules attached via adjacent S atoms, (ii) molecules bound via their outer S atoms and (iii) higher-order peak due to molecular self-assembly.

Sulfur shares this binding characteristic with Au atoms that also preferentially attach to the Al_s sites in the film [27]. The specific Au–oxide interaction has been explained with a charge transfer from the surface Al_s to the Au adatoms, whereby the donated electron is replenished via bond reconfiguration in the oxide lattice combined with the transfer of another electron from the NiAl substrate below. A similar binding mechanism is now proposed for the S atoms in BPPS, which are susceptible to full or partial charge transfer from the oxide cations as well. As discussed in detail for gold, not every Al_s ions in the alumina film is susceptible for charge transfer, because the subsequent bond-reorganization requires the presence of an Al atom in the NiAl directly below the adsorption site [27]. The limited availability of suitable Al_s ions might now explain the unusual binding geometry of BPPS on the alumina film. Apparently, two but not three S atoms are able to interact simultaneously with the surface (Fig. 4a), most likely because the third sulfur always sits in an unfavorable position. Such bidentate binding scheme can indeed be rationalized with the periodicity of the Al_s lattice. The favorable fivefold Al_s ions in pyramidal configuration are spaced either by 10.7, 17.9 or 20.8 Å, according to the short and long axis or the diagonal of the oxide unit cell (Fig. 1a). Whereas the first and last periodicity is indeed found as characteristic spacing between maxima associated with the BPPS molecules, the intermediate distance is rarely observed on the surface. According to the histogram in Fig. 3, a 22 Å-separation between the bound S atoms is most favorable, possibly because the Coulomb repulsion between the sulfur species is minimal and the molecule gains more flexibility to adjust to the oxide film in this binding geometry.

We note that a similar binding scheme could not be developed when the phenyl rings would be imaged in the STM. On the one hand, the attachment of the ad-features to the positively charged Al_s ions in the film could not be explained, as the rings are less susceptible to charge transfer from the oxide. On the other, the anticipated ring diameter would be incompatible with the observed features in the STM that are of atomic dimension. We therefore conclude that the BPPS molecules show up in the STM images mainly through the sulfur atoms that are also responsible for bonding to the oxide film. In contrast, the phenyl

Please cite this article as: Y. Pan, et al., Adsorption of thioether molecules on an alumina thin film, Surf. Sci. (2014), http://dx.doi.org/10.1016/j.susc.2014.05.021

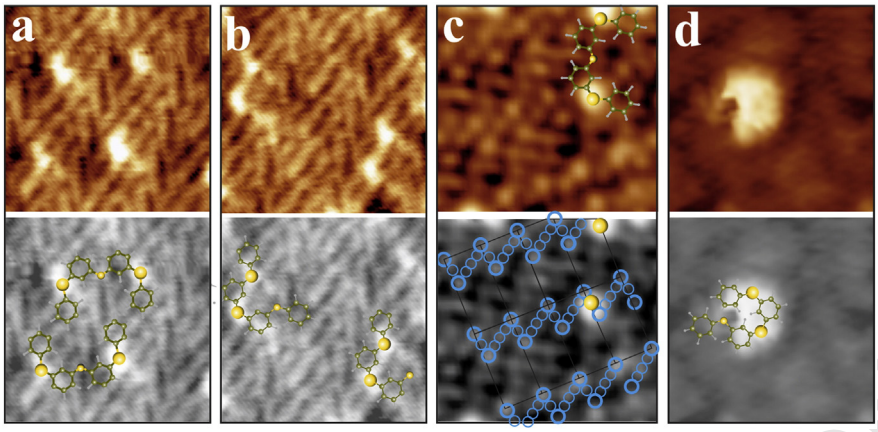

Fig. 4. STM topographic images of two BPPS molecules that bind to the alumina film via (a) the outer and (b) the neighboring S atoms. (c) Single BPPS molecule on an atomically resolved oxide patch. The fivefold coordinated Al_s ions in regular and distorted pyramidal configuration are shown by small and large blue circles, respectively. (d) BPPS species in monodentate binding configuration, in which the molecule revolves around a single surface-sulfur bond acting as anchor site. All structure models in the lower panels are necessarily tentative, as the position of the phenyl rings is not resolved. (For interpretation of the references to color in this figure legend, the reader is referred to the web version of this article.).

rings play only a minor role for adsorption, a conclusion that closely relates to their invisibility in the images. Apparently, the frontier orbitals of the carbon rings are unable to find suitable electronic states for hybridization inside the wide oxide band gap [28]. As a consequence, they are improper final or initial states for tunneling electrons, hence undetectable in the STM [19]. The overlap with the oxide electronic states might be further reduced by a tilting of the phenyl rings against the surface plane. We want to emphasize at this point that our binding model has tentative character as the full molecular configuration cannot be derived from the STM data.

Finally, we discuss the role of intermolecular coupling and possible consequences on the ordering of BPPS species on the alumina film. Although no superstructure is formed, the maxima assigned to the molecular sulfurs typically show a hexagonal arrangement (Fig. 5). The local ordering becomes evident also in the pair correlation function, which exhibits a higher-order peak at 45 Å besides the main maxima at 10 and 22 Å (Fig. 3). A BPPS assembly that would explain this peak is shown in Fig. 5. The molecules are arranged in rows, running along the diagonal of the oxide unit cell, while neighboring rows are displaced by twice the short unit-cell vector (2×10.7 Å). The resulting staggered configuration explains the quasi-hexagonal ordering of the protrusions, as the angle between diagonal and short unit-cell vector amounts to 59°. This arrangement also reproduces the main maxima in the histogram of Fig. 3. While the 22 Å-peak has two origins, the S-S distance in the BPPS and the separation of molecules in two neighboring rows, the maximum at 45 Å reflects the molecular spacing along a row and matches twice the diagonal length of the oxide unit cells (Fig. 5c).

We can only speculate on the nature of the intermolecular interaction that produces this spatial arrangement. The observed spacing is certainly too large to enable direct coupling between the molecules, e.g. via hydrogen bonds formed between S atoms of one and peripheral H atoms of another unit. A template effect of the alumina film is more likely, as already indicated by the matching orientations and distances of the two arrangements. Following our earlier discussion, we propose that only certain positions in the oxide film are able to fix a BPPS molecule at room temperature, such as the distorted pyramidal Al_s ions (dark blue in Fig. 1a). However, most of the molecular degrees of freedom remain active after forming this initial sulfur–Al_s bond and, in particular, the rotation around the anchor site keeps neighboring molecules at distance (Fig. 4d). Only when this motion freezes out upon cooling the sample to 5 K, a second S atom of the BPPS may bind to an adjacent pyramidal Al_s site on the film, orienting the molecule along the diagonal of the oxide unit cell. The observed arrangement can thus be explained with the hexagonal packing of initially rotating BPPS species on the inert surface, and is therefore kinetically driven [29]. We note that other mechanisms might account for the distinct spatial arrangement of thioether molecules on the alumina film, such as their dissociation and/or attachment to surface defects [30]. However, our experiments provide not enough input to validate such binding models at this point. Clarification might be expected either from adsorption experiments performed as a function of temperature or theoretical studies to evaluate different binding geometries. Both approaches are beyond the scope of this paper.

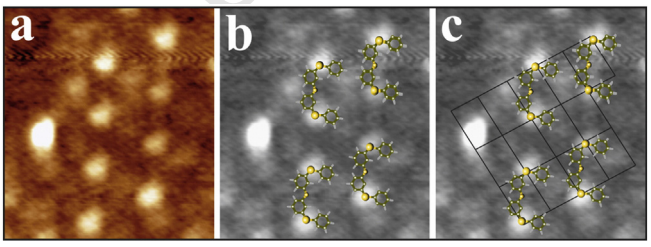

Fig. 5. (a) STM image showing BPPS-related protrusions in a quasi-hexagonal arrangement. (10×10 nm^2, 0.5 V). (b) Same image with a possible configuration of the four BPPS molecules and (c) with the unit-cells of the oxide film. The models are tentative, as the position of the phenyl rings is not resolved.

4. Conclusion

Scanning tunneling microscopy has been used to study the binding of thioether species to a crystalline alumina film. In contrast to metal surfaces, large sections of the molecule remain invisible in the STM, as no hybridization between the molecular LDOS and the oxide states takes place and no transport channels are opened up for the tunneling electrons upon adsorption. Only the sulfur atoms that are directly involved in the binding process produce a topographic fingerprint in the STM. Despite the weakness of the interaction, we successfully developed a binding scenario for BPPS, in which the molecular sulfur attaches to certain Al_s ions in the film while the phenyl rings remain unbound. Our experiments provide new aspects of the interaction between inert oxides and organic molecules, a material combination that is of relevance in Dye-sensitized photovoltaic systems and heterogeneous catalysis.

Acknowledgments

The project has been supported by the COST action CM1104 and the DFG-Cluster of Excellence 'UNICAT'.

References

[1] J.V. Barth, Annu. Rev. Phys. Chem. 58 (2007) 375.
[2] R.K. Smith, P.A. Lewis, P.S. Weiss, Prog. Surf. Sci. 75 (2004) 1.
[3] Z. Ma, F. Zaera, Surf. Sci. Rep. 61 (2006) 229.
[4] A. Hagfeldt, G. Boschloo, L.C. Sun, L. Kloo, H. Pettersson, Chem. Rev. 110 (2010) 6595.
[5] M. Gratzel, J. Photochem. Photobiol. C 4 (2003) 145.
[6] G. Ertl, H. Knoezinger, F. Schueth, J. Weitkamp, Handbook of heterogeneous catalysis, Second ed. Wiley-VCH, Weinheim, 2008.
[7] G. Busca, Catal. Today 27 (1996) 457.
[8] A. Sayari, S. Hamoudi, Chem. Mater. 13 (2001) 3151.
[9] H. Kuhlenbeck, et al., Phys. Rev. B 43 (1991) 1969.
[10] G. Pacchioni, C. Di Valentin, D. Dominguez-Ariza, F. Illas, T. Bredow, T. Kluner, V. Staemmler, J. Phys. Condens. Matter 16 (2004) S2497.
[11] H.J. Freund, H. Kuhlenbeck, V. Staemmler, Rep. Prog. Phys. 59 (1996) 283.
[12] K. Fukui, H. Onishi, Y. Iwasawa, Chem. Phys. Lett. 280 (1997) 296.
[13] N. Ogawa, G. Mikaelian, W. Ho, Phys. Rev. Lett. 98 (2007) 166103.
[14] N. Nilius, V. Simic-Milosevic, J. Phys. Chem. C 112 (2008) 10027.
[15] X. Lin, N. Nilius, J. Phys. Chem. C 112 (2008) 15325.
[16] R.M. Jaeger, H. Kuhlenbeck, H.J. Freund, M. Wuttig, W. Hoffmann, R. Franchy, H. Ibach, Surf. Sci. 259 (1991) 235.
[17] A. Rosenhahn, J. Schneider, C. Becker, K. Wandelt, Appl. Surf. Sci. 142 (1999) 169.
[18] Y. Pan, B. Yang, C. Hulot, S. Blechert, N. Nilius, H.-J. Freund, Phys. Chem. Chem. Phys. 14 (2012) 10987.
[19] B. Yang, Y. Pan, X. Lin, N. Nilius, H.-J. Freund, C. Hulot, A. Giraud, S. Blechert, S. Tosoni, J. Sauer, J. Am. Chem. Soc. 134 (2012) 11161.
[20] G. Kresse, M. Schmid, E. Napetschnig, M. Shishkin, L. Kohler, P. Varga, Science 308 (2005) 1440.
[21] M. Schmid, M. Shishkin, G. Kresse, E. Napetschnig, P. Varga, M. Kulawik, N. Nilius, H.P. Rust, H.J. Freund, Phys. Rev. Lett. 97 (2006) 046101.
[22] J. Libuda, F. Winkelmann, M. Baumer, H.J. Freund, T. Bertrams, H. Neddermeyer, K. Muller, Surf. Sci. 318 (1994) 61.
[23] M. Kulawik, N. Nilius, H.P. Rust, H.J. Freund, Phys. Rev. Lett. 91 (2003) 256101.
[24] N. Nilius, M. Kulawik, H.P. Rust, H.J. Freund, Phys. Rev. B 69 (2004) 121401.
[25] N. Hiroshi, N. Yoshinobu, K. Isao, JP Pat., 10017543 A, (1998) 19980120.
[26] A. Beniya, N. Isomura, H. Hirata, Y. Watanabe, Chem. Phys. Lett. 576 (2013) 49.
[27] N. Nilius, M.V. Ganduglia-Pirovano, V. Brazdova, M. Kulawik, J. Sauer, H.J. Freund, Phys. Rev. Lett. 100 (2008) 096802.
[28] Note that also conductance spectroscopy did not reveal a molecular electronic state in the energy range between −4.0 and +4.0 V.
[29] L. Gao, et al., Phys. Rev. Lett. 101 (2008) 197209.
[30] S.-C. Li, J.-G. Wang, P. Jacobson, X.-Q. Gong, A. Selloni, U. Diebold, J. Am. Chem. Soc. 131 (2009) 980.

Please cite this article as: Y. Pan, et al., Adsorption of thioether molecules on an alumina thin film, Surf. Sci. (2014), http://dx.doi.org/10.1016/j.susc.2014.05.021